

2004

Giant planar Hall effect in colossal magnetoresistive $\text{La}_{0.84}\text{Sr}_{0.16}\text{MnO}_3$ thin films

Y. Bason

L. Klein

J. -B. Yau

X. Hong

C. H. Ahn

Follow this and additional works at: <https://digitalcommons.unl.edu/physicshong>



Part of the [Atomic, Molecular and Optical Physics Commons](#), and the [Engineering Physics Commons](#)

Giant planar Hall effect in colossal magnetoresistive $\text{La}_{0.84}\text{Sr}_{0.16}\text{MnO}_3$ thin films

Y. Bason and L. Klein^{a)}

Department of Physics, Bar Ilan University, Ramat Gan 52900, Israel

J.-B. Yau, X. Hong, and C. H. Ahn

Department of Applied Physics, Yale University, New Haven, Connecticut 06520-8284

(Received 2 December 2003; accepted 5 February 2004)

The transverse resistivity in thin films of $\text{La}_{0.84}\text{Sr}_{0.16}\text{MnO}_3$ (LSMO) exhibits sharp field-symmetric jumps below T_C . We show that a likely source of this behavior is the giant planar Hall effect combined with biaxial magnetic anisotropy. The effect is comparable in magnitude to that observed recently in the magnetic semiconductor Ga(Mn)As. It can be potentially used in applications such as magnetic sensors and nonvolatile memory devices. © 2004 American Institute of Physics.

[DOI: 10.1063/1.1695197]

The planar Hall effect (PHE)¹ in magnetic conductors occurs when the resistivity depends on the angle between the current density \mathbf{J} and the magnetization \mathbf{M} , an effect known as anisotropic magnetoresistance (AMR).² When \mathbf{M} makes an angle θ with \mathbf{J} , the AMR effect is described by the expression $\rho = \rho_{\perp} + (\rho_{\parallel} - \rho_{\perp}) \cos^2 \theta$, where ρ_{\perp} and ρ_{\parallel} are the resistivities for $\mathbf{J} \perp \mathbf{M}$ and $\mathbf{J} \parallel \mathbf{M}$, respectively. The AMR yields a transverse “Hall-like” field if \mathbf{J} is not parallel or perpendicular to \mathbf{M} . Assuming $\mathbf{J} = J_x \hat{x}$ and \mathbf{M} are in the x - y plane with an angle θ between them, the generated electric field has both a longitudinal component:

$$E_x = \rho_{\perp} j_x + (\rho_{\parallel} - \rho_{\perp}) j_x \cos^2 \theta, \quad (1)$$

and a transverse component:

$$E_y = (\rho_{\parallel} - \rho_{\perp}) j_x \sin \theta \cos \theta. \quad (2)$$

This latter component is denoted the planar Hall effect. Unlike the ordinary and extraordinary Hall effects, the PHE shows an even response upon inversion of \mathbf{B} and \mathbf{M} ; therefore, the PHE is most noticeable when \mathbf{M} changes its axis of orientation, in particular between $\theta = 45^\circ$ and $\theta = 135^\circ$.

The PHE in magnetic materials has been previously investigated in 3d ferromagnetic metals, such as Fe, Co, and Ni films, as a tool to study in-plane magnetization.³ It has also been studied for low-field magnetic sensor applications.⁴ Recently, large resistance jumps in the PHE have been discovered in the magnetic semiconductor Ga(Mn)As below its Curie temperature, ~ 50 K.⁵ Four orders of magnitude larger than what has been observed in ferromagnetic metals, it is called the giant planar Hall effect (GPHE). Ga(Mn)As exhibits biaxial magnetocrystalline anisotropy; consequently, the magnetization reversal in a field scan occurs in two steps of 90° rotations. When the current path lies between the two easy axes, the 90° rotations lead to switching-like behavior in the PHE, which is similar to the switching resistivity curves observed in giant magnetoresistance heterostructures⁶ and tunneling magnetoresistance trilayers.⁷ This suggests

that the GPHE in magnetic materials may be suitable for applications in spintronics,⁸ such as field sensors and nonvolatile memory elements.

Here we report on the GPHE observed in the colossal magnetoresistive material (CMR), $\text{La}_{1-x}\text{Sr}_x\text{MnO}_3$ (LSMO). When x is between 0.15 and 0.3, LSMO is a ferromagnetic metal at low temperatures and a paramagnetic insulator at high temperatures, with the Curie temperature coinciding with the metal-insulator transition temperature. Depending on the carrier concentration, the Curie temperature of LSMO ranges from 150 to 350 K. Here, we report on films with a doping level of $x \sim 0.16$ and resistivity-peak temperature of ~ 180 K (see Fig. 1). The films exhibit transverse resistivity jumps comparable to that observed in Ga(Mn)As, and they persist up to temperatures > 140 K.

Thin films (about 40 nm) of LSMO have been deposited epitaxially on single-crystal [001] SrTiO_3 substrates using off-axis magnetron sputtering. θ - 2θ x-ray diffraction reveals c-axis oriented growth (in the pseudo-cubic frame), with a lattice constant of ~ 0.385 nm, consistent with a strained film.⁹ No impurity phases are detected. Rocking curves taken around the 001 reflection have a typical full width at half maximum of 0.05° . The film surface has been characterized using atomic force microscopy, which shows a typical root-mean-square surface roughness of ~ 0.2 nm. The films are patterned into Hall bars using photolithography

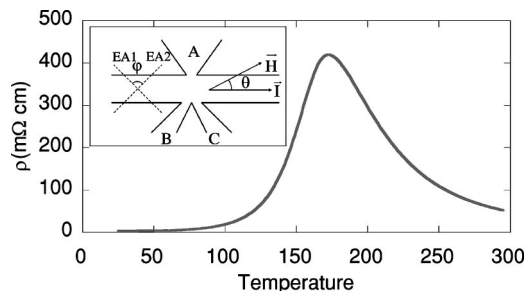


FIG. 1. ρ vs T for an LSMO thin film. Inset: The pattern used for resistivity and Hall measurements. The two easy axes directions (EA1 and EA2) and the angle (θ) between the applied field and the current are also shown. The current path is along either the [100] or [010] direction.

^{a)}Electronic mail: kleinl@mail.biu.aci.il

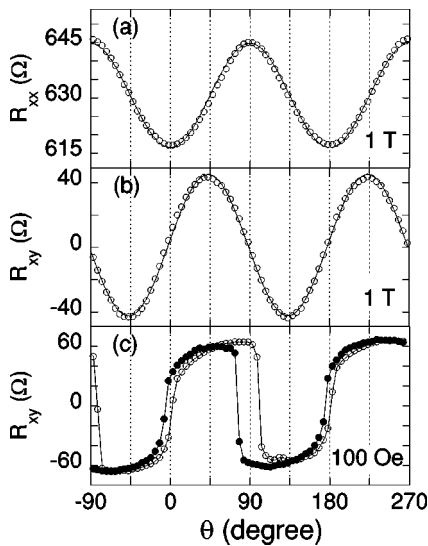


FIG. 2. Measurements of R_{xx} and R_{xy} vs θ at $T=120$ K. (a) R_{xx} measured between B and C. The line is a fit to $\cos^2 \theta$. (b) R_{xy} measured between A and C. The line is a fit to $\sin \theta \cos \theta$. (c) R_{xy} measured between A and C with $H=100$ Oe.

for longitudinal and transverse resistivity measurements (see Fig. 1), with current paths along the [100] and [010] directions.

We first investigate the AMR in the LSMO films with a constant magnetic field applied in the plane of the film. Figure 2 shows the transverse resistivity and the longitudinal resistivity as a function of θ , the angle between the applied magnetic field and the current. The longitudinal resistance, R_{xx} , is measured between B and C (see Fig. 1). The transverse resistance, R_{xy} , is obtained by measuring the resistance between A and C and subtracting the longitudinal component based on the R_{xx} measurement. At high fields the magnetization is expected to be parallel to the applied field. We find that $R_{xx}(\theta)$ has a $\cos^2 \theta$ dependence while $R_{xy}(\theta)$ has a $\sin \theta \cos \theta$ dependence. At lower fields, the angular dependence changes, as the effect of the magnetocrystalline anisotropy becomes significant, and we observe sharp switches in the PHE [see Fig. 2(c)]. We interpret the switches as jumps between easy axes; since the symmetry axes for the switchings are $\theta=0^\circ$ and $\theta=90^\circ$ it is reasonable that the easy axes are in between, namely at $\theta=45^\circ$ and $\theta=135^\circ$.

Figure 3 shows the switching behavior as a function of field sweeps with $\theta=10^\circ$. At high positive field, the magnetization is parallel to the applied field, and the PHE is positive. As the field is reduced, the magnetization gradually aligns along the easy axis closer to the field orientation (EA2). As the field orientation is reversed, the magnetization first switches to the other easy axis (EA1), which is an intermediate state with a negative PHE. As the field becomes more negative, the magnetization goes back to the initial easy axis (EA2), but with opposite polarity. A similar process happens when the field is scanned from negative to positive field.

The temperature dependence of the switching shows that the jumps decrease rapidly as a function of temperature (Fig. 4). Based on the fits to the experimental data (as presented in Fig. 2) and Eqs. (1) and (2), we calculate $\Delta\rho = \rho_{\parallel} - \rho_{\perp}$ at different temperatures. Figure 4 shows $\Delta\rho$ extracted from

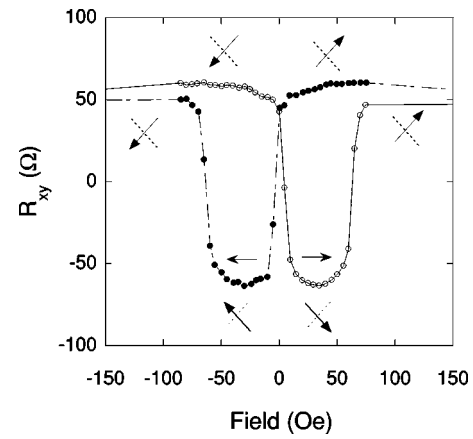


FIG. 3. PHE vs H at 120 K with $\theta=10^\circ$. The arrow shows the magnetization direction along one of the easy axes while the dashed lines indicate the other easy axis direction. The horizontal arrows indicate the field sweep directions.

the AMR ($\Delta\rho_{AMR}$), the PHE ($\Delta\rho_{PHE}$) and the field sweep jump measurements ($\Delta\rho_{jump}$) as a function of temperature. An in-plane magnetic field of 4 T was used to extract $\Delta\rho_{AMR}$ and $\Delta\rho_{PHE}$ at all temperatures. We see that $\Delta\rho_{AMR}$ and $\Delta\rho_{PHE}$ show similar temperature dependencies; however, there is a significant difference in their magnitude.¹⁰ Considering possible sources for this difference, we note that Eqs. (1) and (2) are based on the assumption of uniform current, while the manganites are intrinsically inhomogeneous and exhibit percolative current paths.¹¹ In addition, these equations are expected to be valid for an isotropic medium. Here, the films are epitaxial and the role of crystal anisotropy is yet to be determined.

As shown in Fig. 4, the AMR and GPHE are also observed above T_C , and while switching is naturally not observed, the GPHE may still be interesting for applications where nonhysteretic behavior in field is required, such as Hall sensors.

Biaxial magnetic anisotropy in (001) LSMO films has previously been reported,¹² and there have been studies of biaxial anisotropy¹³ and AMR¹⁴ in other colossal magnetoresistance materials, such as $\text{La}_{1-x}\text{Ca}_x\text{MnO}_3$ (LCMO). Therefore, one may expect to observe the GPHE and switching behavior in CMR materials with other doping levels and chemical compositions.

In conclusion, we have observed the GPHE in LSMO thin films at temperatures as high as 140 K. By optimizing

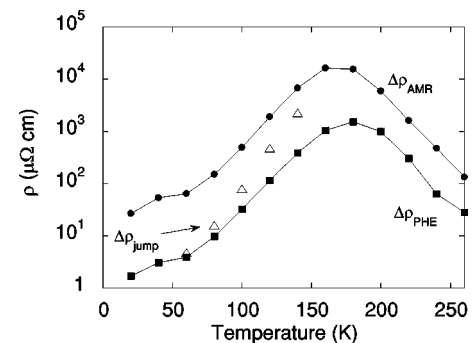


FIG. 4. $\Delta\rho_{AMR}$ (connected circles), $\Delta\rho_{PHE}$ (connected squares)—both measured in a 4 T field, and $\Delta\rho_{jump}$ (unconnected triangles) vs T . $\Delta\rho_{jump}$ is extracted at lower fields. The lines are guide to the eye.

the chemical composition and the device geometry, one may expect a larger effect at higher temperatures, thus allowing for the application of the GPHE in manganites, such as magnetic sensors and non-volatile memory devices.

L.K. and C.H.A. acknowledge support from Grant No. 2002384 from the United States–Israel Binational Science Foundation (BSF), Jerusalem, Israel. L.K. acknowledges support by the Israel Science Foundation founded by the Israel Academy of Sciences and Humanities. Work at Yale supported by AFOSR and NSF.

¹C. Goldberg and R. E. Davis, *Phys. Rev.* **94**, 1121 (1954); F. G. West, *J. Appl. Phys.* **34**, 1171 (1963); W. M. Bullis, *Phys. Rev.* **109**, 292 (1958).

²T. R. McGuire and R. I. Potter, *IEEE Trans. Magn.* **11**, 1018 (1975).

³B. Zhao, X. Yan, and A. B. Pakhomov, *J. Appl. Phys.* **81**, 5527 (1997); A. Nemoto, Y. Otani, S. G. Kim, K. Fukamichi, O. Kitakami, and Y. Shimada, *Appl. Phys. Lett.* **74**, 4026 (1999); G. Li, T. Yang, Q. Hu, H. Jiang, and W. Lai, *Phys. Rev. B* **65**, 134421 (2002); Z. Q. Lu and G. Pan, *Appl. Phys. Lett.* **80**, 3156 (2002); S. Das, H. Yoshikawa, and S. Nakagawa, *J. Appl. Phys.* **93**, 8098 (2003).

⁴A. Schuhl, F. Nguyen Van Dau, and J. R. Childress, *Appl. Phys. Lett.* **66**, 2751 (1995).

⁵H. X. Tang, R. K. Kawakami, D. D. Awschalom, and M. L. Roukes, *Phys. Rev. Lett.* **90**, 107201 (2003).

⁶C. Vouille, A. Barthélémy, F. Elokani Mpondo, A. Fert, P. A. Schroeder, S. Y. Hsu, A. Reilly, and R. Loloee, *Phys. Rev. B* **60**, 6710 (1999).

⁷J. S. Moodera, L. R. Kinder, T. M. Wong, and R. Meservey, *Phys. Rev. Lett.* **74**, 3273 (1995).

⁸S. A. Wolf, D. D. Awschalom, R. A. Buhrman, J. M. Daughton, S. von Molnár, M. L. Roukes, A. Y. Chtchelkanova, and D. M. Treger, *Science* **294**, 1488 (2001).

⁹Y. Moritomo, A. Asamitsu, H. Kuwahara, and Y. Tokura, *Nature (London)* **380**, 141 (1996); H. W. Zandbergen, S. Freisem, T. Nojima, and J. Aarts, *Phys. Rev. B* **60**, 10259 (1999).

¹⁰The difference in the magnitude of $\Delta\rho_{\text{AMR}}$ and $\Delta\rho_{\text{PHE}}$ is also sample dependent.

¹¹For a review see, e.g., E. Dagotto, T. Hotta, and A. Moreo, *Phys. Rep.* **344**, 1 (2001).

¹²L. M. Berndt, V. Balbarin, and Y. Suzuki, *Appl. Phys. Lett.* **77**, 2903 (2000).

¹³J. O'Donnell, M. Onellion, M. S. Rzchowski, J. N. Eckstein, and I. Bozovic, *Phys. Rev. B* **55**, 5873 (1997).

¹⁴J. O'Donnell, J. N. Eckstein, and M. S. Rzchowski, *Appl. Phys. Lett.* **76**, 218 (2000).